Long Range Detection of Emanation from HDMI Cables Using CNN and Transfer Learning

1st Md Faizul Bari
Elmore Family School of ECE
Purdue University
West Lafayette, USA
mbari@purdue.edu

2nd Meghna Roy Chowdhury
Elmore Family School of ECE
Purdue University
West Lafayette, USA
mroycho@purdue.edu

3rd Shreyas Sen
Elmore Family School of ECE
Purdue University
West Lafayette, USA
shreyas@purdue.edu

***Abstract*—The transition of data and clock signals between high and low states in electronic devices creates electromagnetic radiation according to Maxwell's equations. These unintentional emissions, called emanation, may have a significant correlation with the original information-carrying signal and form an information leakage source, bypassing secure cryptographic methods at both hardware and software levels. Information extraction exploiting compromising emanations poses a major threat to information security. Shielding the devices and cables along with setting a control perimeter for a sensitive facility are the most commonly used preventive measures. These countermeasures raise the research need for the longest detection range of exploitable emanation and the efficacy of commercial shielding. In this work, using data collected from 3 types of commercial HDMI cables (unshielded, single-shielded, and double-shielded) in an office environment, we have shown that the CNN-based detection method outperforms the traditional threshold-based detection method and improves the detection range from 4 m to 22.5 m for an iso-accuracy of $\sim 95\%$. Also, for an iso-distance of 16 m, the CNN-based method provides $\sim 100\%$ accuracy, compared to $\sim 88.5\%$ using the threshold-based method. The significant performance boost is achieved by treating the FFT plots as images and training a residual neural network (ResNet) with the data so that it learns to identify the impulse-like emanation peaks even in the presence of other interfering signals. A comparison has been made among the emanation power from the 3 types of HDMI cables to judge the efficacy of multi-layer shielding. Finally, a distinction has been made between monitor contents, i.e., still image vs video, with an accuracy of 91.7% at a distance of 16 m. This distinction bridges the gap between emanation-based image and video reconstruction algorithms.**

***Index Terms*—emanation, electromagnetic compatibility, CNN, transfer learning, ResNet50, HDMI, EMSEC, Signal processing**

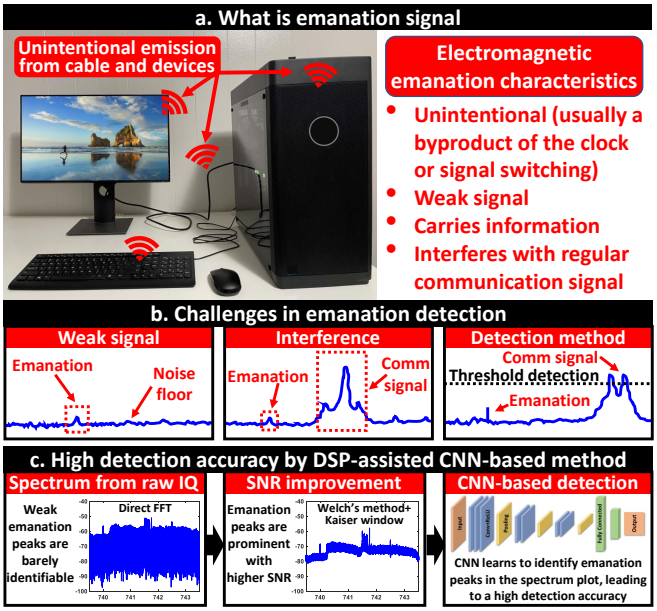

Fig. 1. (a) Emanation is unintentional emission from electronic devices and cables. It is a byproduct of signal switching. (b) The challenges in emanation detection stem from the fact that these are weak signals as they weren't designed to be transmitted. They are often overcast by strong interference from communication signal and performs poorly in the traditional threshold-based detection method. (c) With SNR improvement, tiny emanation peaks become better intelligible. A CNN, trained with the processed power spectrum, can distinguish the emanation peaks from other signals with high accuracy.

I. Introduction

A. Background

Emanation is unintended emission from electronic devices and connecting wires. This type of emission not only creates interference with communication signals (EMI) and electromagnetic compatibility (EMC) problems but also contains a significant correlation with the data being processed in the device, leading to information leakage. It can bypass physical and cryptographic access-to-data control methods at hardware, software, and network levels, forming a 'side-channel' for the attackers leading to several vulnerabilities such as *side-channel attack (SCA)* [1]. Although compromising emanations can be of different types, e.g. electromagnetic, optic, acoustic, ultrasonic, mechanic, etc., electromagnetic emanations are most commonly exploited and widely studied [2].

The exploitation of emanations for eavesdropping has been practiced by military organizations for almost a century. During world war I, the German army used the earth loop current of the allied-force phone line to successfully eavesdrop on their voice communication [3]. The US army investigated the issue in detail during world war II through experimentation at the Bell labs [4]. The codename *TEMPEST* is used to refer to the classified US government program that studies the 'emission security' (EMSEC) issues, possible exploitation, countermeasures, and standardizations (e.g. NATO SDIP-27 Level A, Level B, etc.) [4]. Most information regarding this program is still classified. The first unclassified research paper on emanation

978-3-9819263-7-8/DATE23/© 2023 EDAA

was published by Wim van Eck in 1985 [5]. On a BBC program titled "Tomorrow's world", he demonstrated that the screen content of a display unit can be successfully reconstructed at a long range using very cheap equipment. Electromagnetic emanations are sometimes called 'van Eck radiation' after him [4]. In 2002, a detailed investigation on monitor emanations (both from analog and digital display devices) and screen text reconstruction were performed by Markus G. Kuhn in his doctoral dissertation [2]. Some recent works have exploited monitor and HDMI emanations to reconstruct screen images with text and differently shaped objects [6].

A common method to protect against information leakage via electromagnetic emanations is shielding, which encompasses shielding around a device and/or cables. Also, a control perimeter around a facility is set up. But these approaches raise several research questions such as (i) how effective is commercial shielding around the device or cables? (ii) how long should the control perimeter be? In other words, how far the emanation signals can be successfully detected. To answer these questions, we need to find the maximum detection range using commercially available devices/cables with multiple layers of shielding. There are several challenges in finding the longest detection range. Firstly, emanations are weak signals as they are a byproduct of signal and clock switching, unlike communication signal which is amplified in the power amplifier for transmission. Also, modern devices are comparatively low power, weakening the emanation signals even further. Secondly, they are often detected close to the target device or cable using a sensitive EM probe. But a practical attack scenario would require an antenna with SDR which has lower sensitivity. Thirdly, they don't have an allocated frequency band and are often overshadowed by other signals, making them difficult to detect. Finally, the traditional threshold-based detection method is not very effective in detecting them as they are often weaker than other communication signals in the surroundings. All these challenges may wrongfully create a sense of a shorter detection range than the actual distance up to which they are detectable and exploitable.

In this work, we have focused on emanations from HDMI cables (HDMI 2.0) with different layers of shielding (although classical works focused on emanation from analog display devices, we found that the connecting cable is much louder than modern monitors). Among different types of display cables, we chose HDMI as it is "the most popular cable for monitors today" [7], [8]. We have collected data from HDMI cables of 3 different shielding types (unshielded, single-shielded, and double-shielded) using Ettus B210 SDR as a receiver (RX) in an office environment. We have performed time and frequency domain processing to improve SNR. A CNN (ResNet50) trained with the processed data provides $\sim 100\%$ accuracy up to $16\,\mathrm{m}$ and $\sim 95\%$ accuracy at a distance of $22.5\,\mathrm{m}$ from the target cable, even in the presence of strong interference from other signals. We have explored the effect of multi-layer shielding in HDMI cables. Also, some earlier works have reconstructed static images from monitor emanation while some recent works have performed partial video reconstruction at a short distance. However, these methods assume that the screen is showing solely an image or a video. A method to distinguish between the two types of content will assist the reconstructor to decide which algorithm to run. To that end, exploiting HDMI emanations, we have shown that we can differentiate between static image versus video content with an accuracy of $\sim 91.7\%$ at a distance of $16\,\mathrm{m}$.

B. Our Contribution

- Using 3 types of HDMI cables (unshielded, single shielded, and double shielded) as target and Ettus B210 SDR as RX, **we have collected HDMI emanation data along with background profiling over 3 days from $0.5\ m$ up to $22.5\ m$ in an office environment**.
- Harnessing the power of DSP techniques to improve the SNR and exploiting the advanced image recognition capability of modern CNN, **we have improved the emanation detection range from 4 m to 22.5 m for an iso-accuracy of $\sim 95\%$. Also, $\sim 100\%$ accuracy is achieved up to a distance of 16 m from the target.**
- Comparing the maximum emanation power from HDMI cables with 3 types of shielding, we have **evaluated the efficacy of multi-layer shielding for commercially available cables.**
- **We have distinguished between image vs video emanation signals with an accuracy of $\sim 91.7\%$ at 16 m.**

C. Organization of the Paper

The rest of the paper is structured as follows: section II focuses on relevant works. Section III describes our experimental setup and data collection method. Section IV shows the performance and challenges of traditional threshold-based detection. Section V provides a detailed analysis of performance improvement using the transfer learning approach with ResNet50. It also explores the effect of multi-layer shielding. Section VI shows the performance of still vs video distinction. Finally, section VII concludes the paper with a summary.

II. Related Works

As we have already mentioned, the first publicly available research on compromising emanation was published by Wim van Eck [5] in 1985 based on a CRT monitor. In a technical report based on his Ph.D. dissertation, Markus G. Kuhn explored emanations from both analog (CRT) and digital displays (LCD) [2]. Additionally, he recovered plain text based on radio-character recognition and proposed a civilian radio-frequency emission-security standard [9]. The data for plain-text recovery were collected at a distance of $3\,\mathrm{m}$ from the target monitor. Vulnerability due to emanation from a flat panel display using the digital video interface (DVI) was explored in [10]. Emanation pattern from 4 LCD TV sets was studied and characterized in [11]. Eavesdropping attack on computer displays with success to some extent has been shown in [12].

In [13], emanations from a video graphics array (VGA) cable are collected using an EM probe and oscilloscope. Exploiting this emanation, the authors recovered the outline of the screen text [13] and some noisy shapes [14]. A different type of

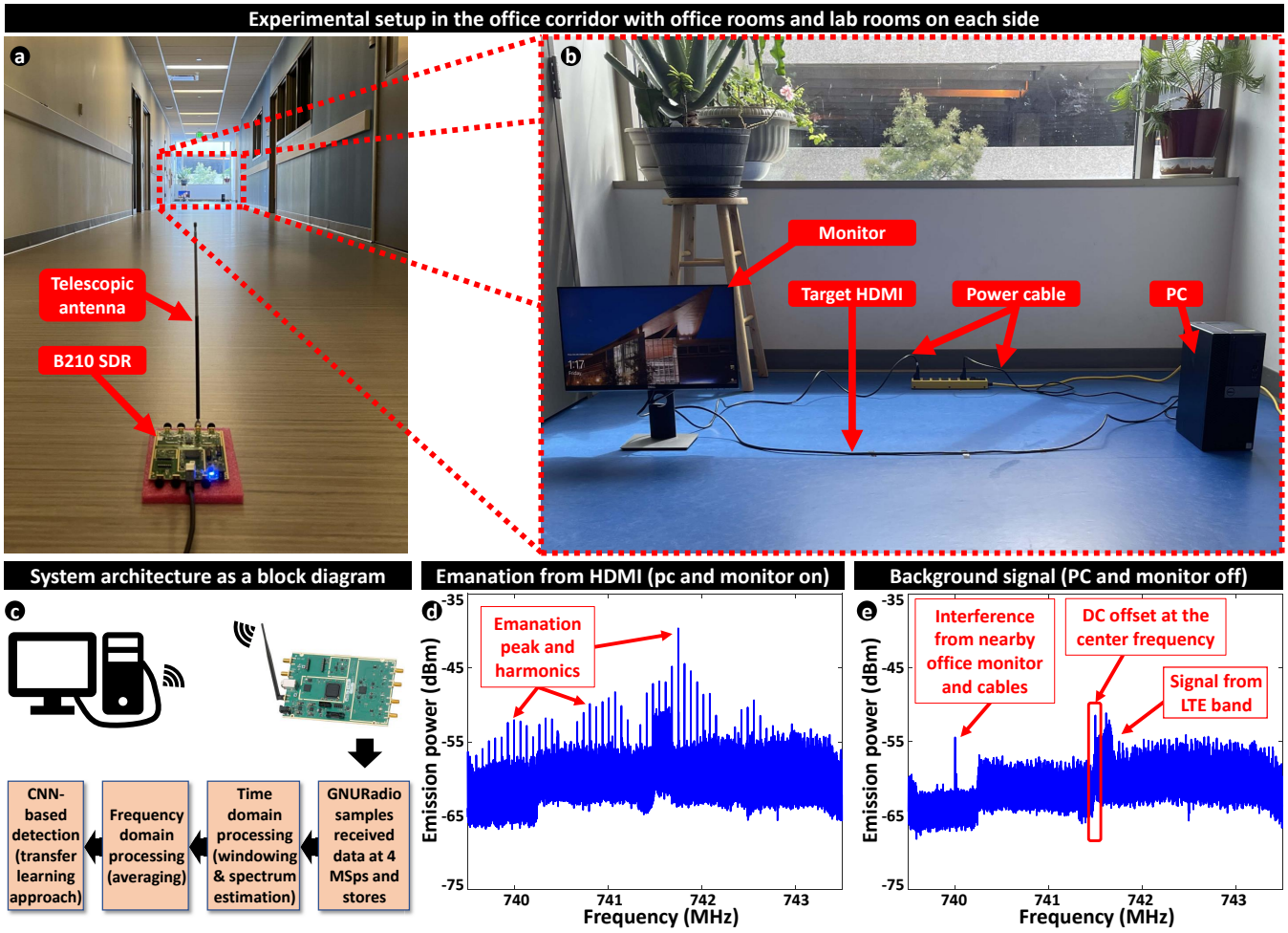

Fig. 2. (a) Physical setup in the office corridor using Ettus B210 SDR (connected to a wideband telescopic antenna) as a receiver. (b) The target HDMI is connected between a PC and a monitor. (c) Full system architecture. GNURadio interface samples the received data at 4 MSps which are processed both in the time and frequency domain. A CNN (ResNet50) is trained with this data. (d) Emanation peak and harmonics from an unshielded HDMI cable. (e) The background signal contains strong interference from nearby office equipment and LTE band. Also, SDR adds a DC offset at the center frequency.

analysis was published in [15], where the authors compared emanations in terms of the most common display interfaces: DVI and DisplayPort. Collecting data in an anechoic chamber at a distance of $1\,\mathrm{m}$, the authors reconstructed texts displayed on the screen for both of them and concluded that DisplayPort was safer in terms of leakage. In [16], the authors have used several techniques such as vertical and horizontal frame synchronization, multi-frame averaging, skew correction, etc. to improve the quality of the reconstructed image. Both DVI and HDMI use the 'transition-minimized differential signaling (TMDS)' protocol [17]. Recent work has shown a quantitative analysis of compromising emanation from the TMDS interface and possible exploitation [18].

III. Data Collection

A. Experimental Setup

Fig. 2(a) shows our experimental setup in an office corridor. Fig. 2(b) shows a zoomed-in view of the target HDMI, connecting a LED monitor (Dell P2319H) and a PC. As RX, we have used Ettus B210 SDR connected with a wideband telescopic antenna as shown in Fig. 2(a). A GNURadio interface collects the received data, samples at $4\,\mathrm{MS/sec}$ and stores them. These are processed using both time and frequency domain SNR improvement techniques and finally fed to a ResNet50. This whole system architecture is shown in Fig. 2(c).

B. Emanation Data Capture

To choose the center frequency (CF) for data collection, we initially used a spectrum analyzer to scan from DC to $4\,\mathrm{GHz}$. Our scan shows Sinc-train over a wide band but the strongest peak was near $742\,\mathrm{MHz}$. Since SDRs often have DC offset at CF, we chose $742.5\,\mathrm{MHz}$ as our CF so that the $742\,\mathrm{MHz}$ peak doesn't merge with the DC offset. Three different types of cables have been used: unshielded, single-shielded, and double-shielded. For each cable, we have collected data from $0.5\,\mathrm{m}$ to $22.5\,\mathrm{m}$, at $0.5\,\mathrm{m}$ intervals. Fig. 2(d) shows the emanation signal in the frequency domain for an unshielded HDMI cable at $1\,\mathrm{m}$.

C. Background Profiling

Background profiling is a very crucial part of data collection as it keeps changing. To keep the profile as fair as

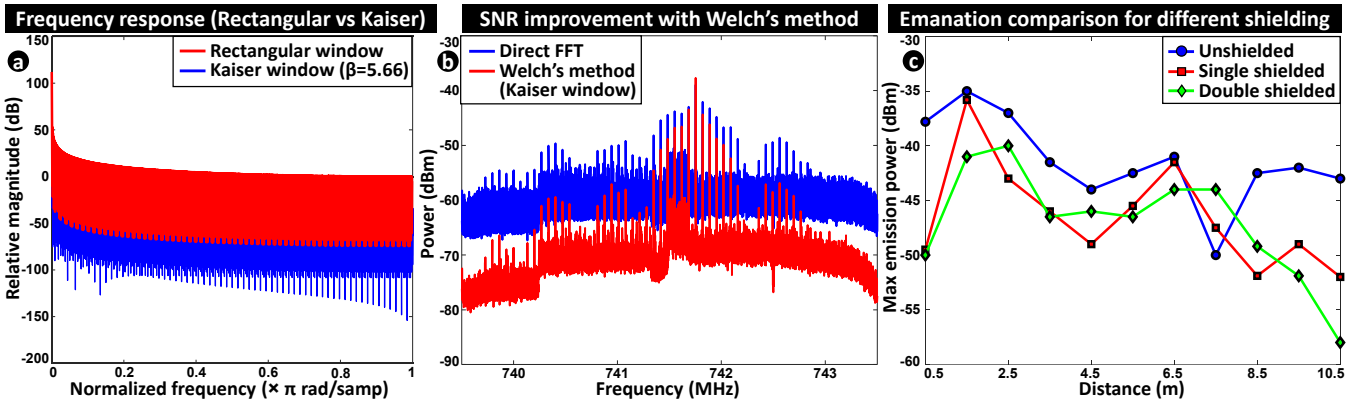

Fig. 3. (a) Frequency response of rectangular and Kaiser windows shows much less spectral leakage for the latter. (b) Using Welch's method of power spectrum estimation (along with Kaiser window), we get $\sim 15\,\mathrm{dB}$ SNR improvement. (c) Comparison of 3 types of HDMI (unshielded, single-shielded, and double-shielded) in terms of maximum emanation power. The unshielded cable is much louder in most cases while the difference between the other two is trivial.

possible, we have collected background data on 3 separate days at 3 separate times: in the morning, at noon, and night. Fig. 2(e) shows a sample background spectrum. Our target frequency ($742.5\,\mathrm{MHz}$) falls in the LTE band (lower SMH block, $729\,\mathrm{MHz}$ to $746\,\mathrm{MHz}$). Fig. 2(e) clearly shows the LTE signal energy. Also, there are multiple experimental labs along with student and staff office rooms on both sides of the corridor, contributing to some additional interference. Also, we can see DC offset at the center.

IV. Threshold-Based Detection

A. Detection Method

Threshold-based peak detection is widely used in literature, including some recent ones [19]. The collected I-Q data are transformed into the frequency domain via FFT and compared against a threshold level. If there is a power peak above the threshold, we detect the presence of an emanation signal.

TABLE I
Performance Analysis of Threshold-Based Detection

Threshold (dBm)	FP (%)	FN (%)	Accuracy (%)
-45	0	74.07	62.96
-55	26.67	15.56	78.89
-65	100	0	50

However, the accuracy is dependent on the threshold. If the threshold is too high, there will be a lot of false-negative (FN), whereas too low threshold will result in a lot of false-positive (FP) data. We have tested the detection performance of our dataset for 3 threshold levels. Table I shows that the $-55\,\mathrm{dB\,m}$ threshold provides the best accuracy, which is still pretty low.

B. Challenges

Table I shows that threshold-based detection does not perform well (best-case accuracy $< 80\%$). There are several reasons for that. The key issue is the strong interference from other signals (LTE signals, emanations from other cables, etc.). These peaks in the background are falsely detected as emanation for low thresholds, leading to high FP values. On the other hand, raising the threshold does not help much as emanation signals are weak themselves and cannot cross the high threshold bar. This leads to high FN values. Also, the background noise level keeps changing based on the environment. This poses a challenge for adaptive threshold selection. Another issue is the peak at the center frequency due to DC offset. To address these issues, we resort to CNN-based detection.

V. Performance Improvement using CNN

A. SNR Improvement using DSP Techniques

Before training a CNN, we want to improve the perceived SNR of the collected signal. To that end, we apply some known techniques in the DSP domain.

1) Windowing in Time Domain: Our data is finite in the time domain, which is equivalent to applying a rectangular window to an infinite time sequence of data. However, the rectangular window has a significant spectral leakage from the main lobe to the side lobe [20]. There are better windows (Hanning, Hamming, Kaiser, etc.) with lower spectral leakage. The downside is the larger main lobe width. However, the main lobe width is inversely proportional to the data length and we have significantly long data to overcome this limitation.

Fig. 3(a) shows the frequency response of a rectangular window and a Kaiser window ($\beta = 5.66$). The spectral leakage for the Kaiser window is only 0.01% compared to 9.28% for the rectangular window. Also, relative side-lobe attenuation reduces from $-13.3\,\mathrm{dB}$ to $-41.4\,\mathrm{dB}$. We have windowed our data with the designed Kaiser window ($\beta = 5.66$).

2) Power Spectrum Estimation using Welch's Method: We have used Welch's method of power spectrum estimation (modified periodogram with averaging) as a better spectrum estimate. A sequence of 4×10^5 samples ($0.1\,\mathrm{s}$ data) is taken and divided into 8 segments with 50% overlap. A modified periodogram (FFT of autocorrelation, instead of direct FFT) is applied to each segment and the output is averaged. Fig. 3(b) compares the spectrum of I-Q data corresponding to emanations from unshielded HDMI cable at $1\,\mathrm{m}$ distance, found using direct FFT and Welch's method. It is shown that the maximum peak is similar for both, but the noise level is reduced. We gain $\sim 15\,\mathrm{dB}$ SNR improvement.

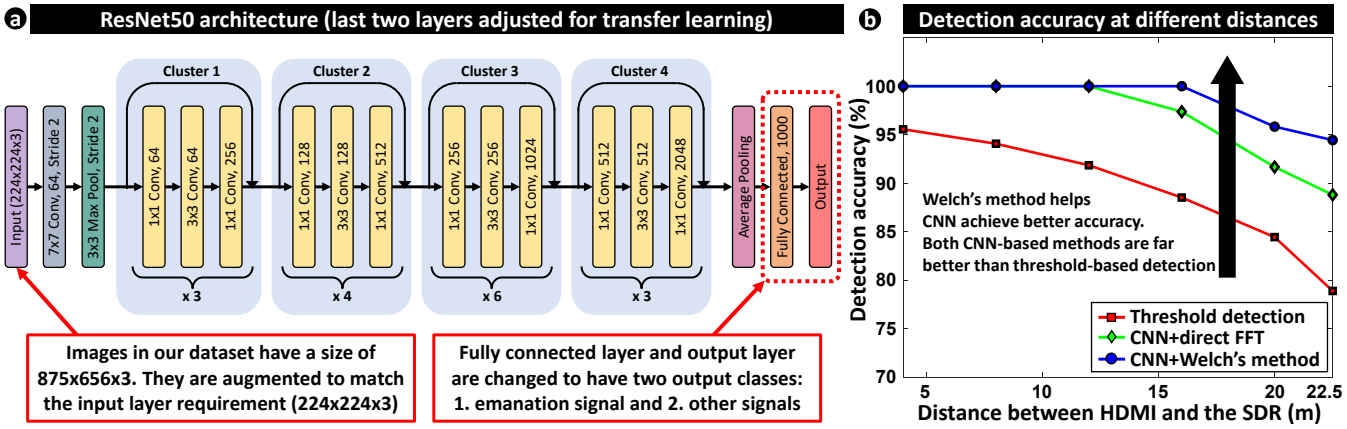

Fig. 4. (a) ResNet50 architecture. Images in our dataset are augmented to match the input size (224x224x3). The fully connected layer and the output layer are modified to classify two groups: emanation vs every other signal. (b) Performance comparison between threshold-based detection (in the best case at -55 dBm threshold) and CNN-based detection (both for direct FFT and Welch's method). SNR improvement provides a better detection range for iso-accuracy and better accuracy for iso-distance compared to FFT from raw data. In both cases, the CNN-based method outperforms the threshold-based method by a high margin.

3) Averaging in Frequency Domain: Frequency domain averaging reduces noise power, keeping the signal peaks almost intact. We apply Welch's method for 9 consecutive sequences with 50% overlap in the time domain. The spectrums of the sequences are averaged to reduce the noise power.

B. Effect of Multi-Layer Shielding on Emanation

After improving the SNR, we want to check the efficacy of multi-layer shielding before moving on to training CNN. Fig. 3(c) shows the emanation power for 3 types of HDMI cables from 0.5 m to 10.5 m at 1 m intervals. Except for a few outliers, the maximum emanation power for the unshielded cable (blue line) is significantly higher than the other two, which is expected. However, the difference between the single and double-shielded cables is trivial.

C. Transfer Learning using ResNet50

Our final step is to evaluate the performance of the CNN-based detection method. For that, we have used transfer learning approach where a widely used, pretrained CNN (e.g. VGG16 [21], AlexNet [22], GoogLeNet [23], ResNet50 [24], etc.) is retrained [25], [26] with a new dataset. These networks are carefully designed and reviewed by experts in the field and are known to classify images in standard datasets (e.g. ImageNet) with high accuracy. Our initial testing shows that ResNet50 works best for our case.

Fig. 4(a) shows the ResNet50 architecture. Residual Neural Network or ResNet revolutionized the use of the ultra-deep network by using 'skip connection' to address the issue of 'vanishing gradient' and 'degradation problem'. It performed much better compared to VGG or GoogLeNet on the 'ImageNet dataset' [27]. We will exploit the enhanced image classification capability of ResNet50 for our dataset. For training purposes, we have used the frequency domain plots as images. The rationale behind using the plots instead of the 1D sequence is to exploit the advanced image classification capability of CNN (ResNet50). Our images are augmented to match the input size. The fully connected layer and the output layer are adjusted for binary classification (emanation vs others). The train, test, and validation data ratio was 70:20:10. We have used an initial learning rate = 0.001, mini-batch size = 8, and max epoch = 30. Data are shuffled at each epoch.

D. Performance Evaluation

Fig. 4(b) shows the performance of ResNet50 via transfer learning for a distance of 4 m to 22.5 m. For data with better SNR (thanks to Welch's method), we get $\sim$ 100% accuracy up to 16 m which gradually reduces to $\sim$ 95% at 22.5 m. This figure also compares the performance benefit with improved SNR. Compared to direct FFT, we get a longer distance for iso-accuracy (e.g. for 100% accuracy, we get 16 m compared to 12 m) and higher accuracy for the same distance (e.g. at 22.5 m, we get $\sim$ 95% accuracy compared to $\sim$ 88.9%). In both cases, the CNN-based method outperforms the threshold-based method by a high margin.

E. Performance Comparison

Earlier works focused on the screen content recovery instead of the detectable range. Hence, a comparison with this work is not exactly apple to apple. Nonetheless, a list of data collection ranges is provided in Table II for interested readers.

TABLE II
PERFORMANCE COMPARISON WITH PREVIOUS WORKS

Display emanation study	Detection range (m)
Text recovery from flat-panel display [10]	10
Information recovery from LCD monitor [16]	3
Proposed method (this work)	22.5

VI. Monitor Content Type Detection - Still vs Video

A. Motivation

In the literature review section, we have discussed that some works have reconstructed screen images with plain text and some geometric shapes. Some recent works have tried to

reconstruct video signals. However, these works assume that the monitor is running solely a video or just an image. An automated method is necessary to detect the content type of the monitor (still image vs video) and switch to the corresponding detection algorithm. In this subsection, we try to fill that void.

B. Performance Evaluation

Our data collection method is the same as before, except that a video was playing on the monitor. The emanation signal captures the changes due to the video playback. We have used the same data processing steps before training ResNet50 with the data to check whether it can distinguish between the two. Our evaluation shows that we get 91.7% accuracy at a distance of $16\,\mathrm{m}$ which gradually drops at a further distance.

VII. Conclusion

In this work, we have collected emanation data from 3 types of HDMI cables in an office environment for distances covering up to $22.5\,\mathrm{m}$. Training ResNet50 with the spectrum achieved using direct FFT, we have been able to attain $\sim 100\%$ accuracy up to $12\,\mathrm{m}$, which gradually drops to $\sim\ 88.9\%$ at $22.5\,\mathrm{m}$. The CNN-based detection method outperforms the traditional threshold-based detection method. Using windowing, a better power spectrum estimation, and averaging, the SNR of the signal is improved which boosts the performance of the CNN to the next level to provide $\sim 100\%$ accuracy up to $16\,\mathrm{m}$ and $\sim 95\%$ accuracy at $22.5\,\mathrm{m}$. To the best of our knowledge, this is the highest detection range for HDMI emanation ever reported in the literature. The emanation power of the 3 types of cable is compared and matched with the theoretically expected value. Finally, collecting data for emanation when a video is being played, it is shown that a distinction can be made between still image and video with 91.7% accuracy at $16\,\mathrm{m}$. These results show the performance benefit of CNN-based emanation detection and signal type classification which paves the way for AI-assisted image and/or video reconstruction in the future.

Acknowledgment

This research was supported by the Office of the Director of National Intelligence (ODNI), Intelligence Advanced Research Projects Activity (IARPA), via contract: 2021-21062400006. The views and conclusions contained herein are those of the authors and should not be interpreted as necessarily representing the official policies or endorsements, either expressed or implied, of the ODNI, IARPA, or the U.S. Government. The U.S. Government is authorized to reproduce and distribute reprints for Governmental purposes not withstanding any copyright annotation thereon.

References

[1] M. Randolph and W. Diehl, "Power Side-Channel Attack Analysis: A Review of 20 Years of Study for the Layman," Cryptography, 2020, vol. 4, no. 2, p. 15, doi: 10.3390/cryptography4020015.

[2] M. G. Kuhn, "Compromising emanations: eavesdropping risks of computer displays," (Doctoral dissertation, University of Cambridge), 2002.

[3] J. Young. "How Old is Tempest?." https://cryptome.org/tempest-old.htm (Accessed Jan. 25, 2023).

[4] "Tempest (codename)," Wikipedia. https://en.wikipedia.org/wiki/Tempest_(codename). (Accessed Jan. 25, 2023).

[5] W. Van Eck, "Electromagnetic radiation from video display units: An eavesdropping risk?," Computers & Security 4, no. 4 ,1985, 269-286.

[6] H. S. Lee, D. H. Choi, K. Sim and J. -G. Yook, "Information Recovery Using Electromagnetic Emanations From Display Devices Under Realistic Environment," in IEEE Transactions on Electromagnetic Compatibility, vol. 61, no. 4, pp. 1098-1106, 2019, doi: 10.1109/TEMC.2018.2855448.

[7] L. Knerl. "What are the most popular computer monitor cable types?," HP.com. https://www.hp.com/us-en/shop/tech-takes/most-popular-computer-cable-types (Accessed Jan. 25, 2023)

[8] "Different types of monitor cables - blog: SF Cable," Sfcable.com. https://www.sfcable.com/blog/types-monitor-cables-2. (Accessed Jan. 25, 2023).

[9] M. G. Kuhn, "Security limits for compromising emanations," in International Workshop on Cryptographic Hardware and Embedded Systems, 2005, pp. 265-279.

[10] M. G. Kuhn, "Electromagnetic eavesdropping risks of flat-panel displays," in International Workshop on Privacy Enhancing Technologies,2004, pp. 88-107. doi: https://doi.org/10.1007/11545262_20

[11] M. G. Kuhn, "Compromising emanations of LCD TV sets," in IEEE Transactions on Electromagnetic Compatibility, 2013, 55, no. 3 ,pp 564-570. doi: 10.1109/TEMC.2013.2252353.

[12] M. G. Kuhn, "Eavesdropping attacks on computer displays," in Information Security Summit, 2006, 24-25.

[13] H. S. Lee, J. -G. Yook and K. Sim, "Measurement and analysis of the electromagnetic emanations from video display interface," in IEEE Electrical Design of Advanced Packaging and Systems Symposium (EDAPS), 2015, pp. 71-73, doi: 10.1109/EDAPS.2015.7383670.

[14] H. S. Lee, J. -G. Yook and K. Sim, "An information recovery technique from radiated electromagnetic fields from display devices," in Asia-Pacific International Symposium on Electromagnetic Compatibility (APEMC), 2016, pp. 473-475, doi: 10.1109/APEMC.2016.7522772.

[15] I. Kubiak and A. Przybysz, "DVI (HDMI) and DisplayPort digital video interfaces in electromagnetic eavesdropping process," in International Symposium on Electromagnetic Compatibility - EMC EUROPE, 2019, pp. 388-393, doi: 10.1109/EMCEurope.2019.8872097.

[16] H. S. Lee, D. H. Choi, K. Sim and J. -G. Yook, "Information Recovery Using Electromagnetic Emanations From Display Devices Under Realistic Environment," in IEEE Transactions on Electromagnetic Compatibility, vol. 61, no. 4, pp. 1098-1106, Aug. 2019, doi: 10.1109/TEMC.2018.2855448.

[17] "Transition-minimized differential signaling," Wikipedia.com. https://en.wikipedia.org/wiki/Transition-minimized_differential_signaling . (Accessed Jan. 25, 2023).

[18] E. Lee, D. -H. Choi, T. Nam and J. -G. Yook, "A Quantitative Analysis of Compromising Emanation From TMDS Interface and Possibility of Sensitive Information Leakage," in IEEE Access, 2022, vol. 10, pp. 73997-74011, doi: 10.1109/ACCESS.2022.3184294.

[19] M. F. Bari, M. R. Chowdhury, B. Chatterjee and S. Sen, "Detection of Rogue Devices using Unintended Near and Far-field Emanations with Spectral and Temporal Signatures," in IEEE/MTT-S International Microwave Symposium - IMS, 2022, pp. 591-594, doi: 10.1109/IMS37962.2022.9865347.

[20] J. G. Proakis and D. G. Manolakis, "Digital Signal Processing: Principles, algorithms, and applications," 3rd ed. Upper Saddle River, NJ: Pearson Prentice Hall, 2007.

[21] K. Simonyan, and Z. Andrew, "Very deep convolutional networks for large-scale image recognition," in arXiv preprint, 2014, arXiv:1409.1556.

[22] A. Krizhevsky, S. Ilya, and H.E. Geoffry, "Imagenet classification with deep convolutional neural networks," in Communications of the ACM, 2012, 60(6), 84-90.

[23] C. Szegedy, et al. "Going deeper with convolutions." IEEE Conference on Computer Vision and Pattern Recognition (CVPR), 2015, pp. 1-9, doi: 10.1109/CVPR.2015.7298594.

[24] K. He, X. Zhang, S. Ren and J. Sun, "Deep Residual Learning for Image Recognition," in IEEE Conference on Computer Vision and Pattern Recognition (CVPR), 2016, pp. 770-778, doi: 10.1109/CVPR.2016.90.

[25] "Transfer learning," Wikipedia, 22-Jul-2022. [Online]. Available: https: en.wikipedia.org/wiki/Transfer_learning. (Accessed Jan. 25, 2023).

[26] L. Torrey and S. Jude, "Transfer learning," in Handbook of research on machine learning applications and trends: algorithms, methods, and techniques, IGI global, 2010, pp. 242-264.

[27] I. Rajagopal, "Intuition behind residual neural networks," Medium, 22-Jul-2020. [Online]. Available: https://towardsdatascience.com/intuition-behind-residual-neural-networks-fa5d2996b2c7. (Accessed Jan. 25, 2023).